

# Characterization of the effect of helicopter isolated blade vortex on dynamic stall

Farid Hosseinzadeh Esfahani<sup>1</sup>, Seyed Mohammad Hossein Karimian<sup>1\*</sup>, Hamid Parhizkar<sup>2</sup>

<sup>1</sup> Department of Aerospace Engineering, Amirkabir University of Technology, Tehran, Iran.

<sup>2</sup> Department of Aerospace Engineering, Malek Ashtar University of Technology, Tehran, Iran.

## ABSTRACT

In this research, dynamic stall at sections near the rotor blade tip at maximum cruise speed of the helicopter with an advanced ratio of 0.35 and cyclic pitching motion, has been studied using CFD simulation. URANS equations are solved using  $k - \omega$  SST model on a domain discretized into a hybrid mesh using finite volume discretization method. Numerical simulation is validated using experimental results of AH1-G helicopter flight tests. Comparison of results indicates that present numerical results match with experimental data well. Dynamic stall occurs as a result of shock wave in the advancing side which affects lift coefficient. Interestingly, the effect of shock wave on the lift coefficient in the regions closer to the blade tip is weakened due to the tip vortex penetration. As a result, few changes are seen in the lift coefficient in these regions in comparison to those of the inner regions of the blade. In addition, the maximum value of lift coefficient in the section closer to the blade tip reduces by 10.2% in comparison to that of most inner section. Results show that despite the formation of the leading-edge vortex, especially in the inner most sections of the blade, severe dynamic stall does not occur in the retreating side. Infact, this is due to the weakening of the leading edge vortex by the effect of the radial flow.

## KEYWORDS

Dynamic stall, Unsteady separation, Helicopter aerodynamics, Leading edge vortex, Trailing edge vortex

---

\* Corresponding Author: hkarim@aut.ac.ir

## 1. Introduction

The complexity of fluid flow around the rotor blade in forward flight limits helicopter's flight envelop. These complexities include time-varying pitch angle, mechanical out of plane motion, compressibility, unsteady boundary layer, large scale flow separations, dynamic stall, and reverse flow area. The mechanism of dynamic stall phenomenon and the parameters affecting it, have been among the interesting research topics in experimental and numerical aerodynamics for many years. Experimental results of pitching airfoils in retreating side under dynamic stall have been published by Ham et al. [1, 2] and Mc Crosskey et al.[3].

In this paper, the primary objective is to investigate three dimensional characteristics of dynamic stall vortex formation at the three radial sections of blade close to the blade tip at the maximum allowable cruise speed. Due to the flight envelope of helicopter speed in relation to compressibility and dynamic stall, the study of this speed is particularly important in the design of the rotor blade.

## 2. Methodology

### 2-1. Governing Equations and Numerical Modeling

In this paper, equations are solved using pressure-based solver with second-order upwind discretization for the convection terms and second-order implicit discretization for the transient terms. Also, a two equation  $k-\omega$  SST model is utilized to capture the effect of turbulent flow.

### 2-2. Blade Geometry and Computational Domain

Geometry of the rotor blade used here has a radius of 5.5 meters from the center of rotation. It has two parts with different types of airfoil profiles (NACA23012 and NACA13008) and a third part to provide transition between these two parts. Flow conditions and blade's control variables at maximum flight speed are shown in Table 1.

**Table 1. Flight condition and blade control variables**

Parameters	Value
$M_{Tip}$	0.65
$M_{\infty}$	0.236
$\mu$	0.35
$\theta_0$	13.89
$\theta_{lc}$	1.34
$\theta_{ls}$	-5.71
$\Omega$	40.3

Computational domain is formed from three different mesh regions. A rigid mesh like a capsule is created around the blade from the root to the tip to facilitate blade pitching motion. To provide rotor rotation, this capsule-like mesh is located in a cylindrical mesh which rigidly rotates with the speed of the rotor. This cylindrical mesh itself is located within a stationary spherical mesh to represent the outer far field. Cyclic pitch of blade is applied by equation (1).

$$\theta = \theta_0 + \theta_{lc} \cos \psi(t) + \theta_{ls} \sin \psi(t) \quad (1)$$

where  $\theta_0$  is the collective pitch angle,  $\theta_{lc}$  is the lateral cyclic pitch,  $\theta_{ls}$  is the longitudinal cyclic pitch angle, and  $\psi(t)$  denotes the azimuth angle.

### 2-4. Validation and Verification

Simulation results are validated and verified using the flight test data and numerical simulation results of the AH-1G helicopter at a maximum flight speed of 159 knots performed by Tejero Embuena et. al. [4], respectively.

Figure 1 depicts comparison of the present results of normal force coefficient at one section in the dimensionless radius ( $r/R$ ) of 0.86 with those of the flight test data and numerical results of FLOWer solver.

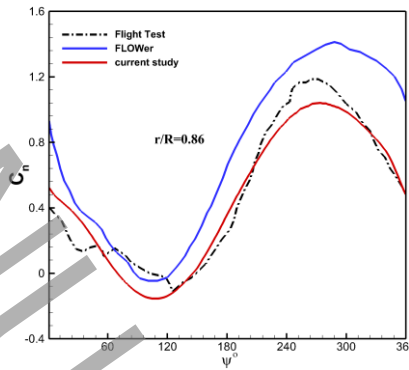


**Fig 1. Comparison of the present numerical results of normal force coefficient with those of the flight test data and numerical results for AH-1G helicopter**

Present results compare well with those of flight test in figure 1. The maximum difference between the normal force coefficient obtained in this study and that of experimental data was 12%, which occurs at azimuth angle of 269 degrees in the third quarter of the blade rotation. Present numerical results demonstrate that the simulation is done correctly in this research study. As seen, in comparison to the numerical results of FLOWer present results are closer to the experimental data.

### 3. Results and Discussion

To better understand the behavior of dynamic stall and high flow separations on the rotor blade with cyclic pitch, three sections in dimensionless radial positions ( $r/R$ ) of 0.778, 0.85 and 0.95 close to the blade tip are investigated. Variation of lift coefficient with azimuth angle in these three sections are shown in Figure 2. For section with  $r/R=0.778$ , maximum of lift coefficient occurs at the azimuth angle of 39 degrees and after that the lift coefficient suddenly drops. This is due to shock-induced separation. At this azimuth angle, the maximum Mach number of this section is 1.32. Similarly, in sections with  $r/R=0.85$  and 0.95 shock-induced separation occurs at the azimuth angles of 23 and 17 degrees respectively.

Due to the three-dimensional effects of attenuated tip vortex penetration, effect of shock wave on lift coefficient in regions closer to the blade tip decreases as seen in figure 2. In addition, variation of lift coefficient at section near the blade tip have become more smooth. As a result, the ratio of lift coefficient to its maximum value at section with  $r/R=0.95$  has decreased by 10.2% in comparison to that of section  $r/R=0.778$ . In the third quadrant of the blade rotation, the lift coefficient experiences another abrupt drop at the azimuth angle of 205 degrees on the section  $r/R=0.778$ . The same happens at the section with  $r/R=0.85$  at azimuth angle of 171 degrees. At the section with  $r/R=0.95$ , no sudden change is seen in second and third quadrants. by moving in time, In the fourth quadrant of the blade rotation, section 0.778 has two sharp drops in its lift coefficient. The first drop is from 322 to 337 degrees and the next drop that is more severe, is from 343 to 360 degrees. At the section with  $r/R=0.85$ , there is a sharp drop in lift coefficient at an angle of 297 to 340 degrees. At the section with  $r/R=0.95$ , however, there is no sudden drop in this range of motion and the lift coefficient gradually decreases.

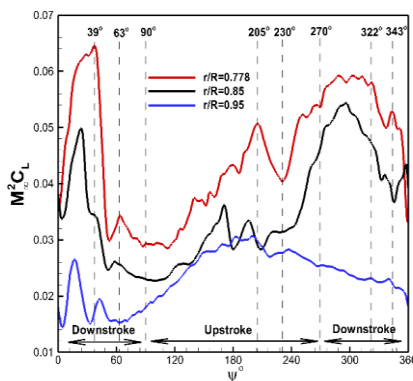


Fig 2. Lift coefficient variation with azimuth angle for section 0.778, 0.85, and 0.95

### 4. Conclusions

In this research, numerical simulation of the helicopter rotor blade with cyclic pitching has been performed at the maximum cruise speed to understand its flow complexities at the three selected sections in the region close to the blade tip by the finite volume method. Numerical results obtained here showed that

- 1) The reason for the occurrence of dynamic stall on all three blade sections in the first quadrant of rotor rotation, where the relative speed of flow with respect to the blade section is high, is the shock-induced separation.
- 2) As a result of relatively high-speed rotor rotation, strong radial flow is formed towards the blade tip. Despite the growth of dynamic stall vortex this radial flow pushes these vortices towards the blade tip and prevents them from sufficient growth and durability. Therefore, limited dynamic stall occurs at the inner sections. At section with  $r/R=0.778$  dynamic stall occurs in the third and fourth quadrants. This is accompanied by the growth of the TEV and the weakening of the LEV. Also, at the section with  $r/R=0.85$ , formation of a weaker dynamic stall is observed in third quarter of the rotor blade rotation.
- 3) Despite the existence of extensive flow separation at the third section where  $r/R=0.95$ , strong penetration of the tip vortex and its effect on the LEV dynamic stall does not occur at all.

The results of the present study can be used to design the geometry of the tip shape and according to the effects of the vortex penetration on the dynamic stall conditions of the outer blade area, it can be used as a factor limiting the maximum allowable flight speed in helicopters.

### 5. References

- [1] N.D. Ham, Aerodynamic loading on a two-dimensional airfoil during dynamic stall, AIAA journal, 6(10) (1968) 1927-1934.
- [2] N.D. Ham, M.S. Garelick, Dynamic stall considerations in helicopter rotors, Journal of the American Helicopter Society, 13(2) (1968) 49-55.
- [3] W. McCroskey, R. Fisher, Dynamic stall of airfoils and helicopter rotors, AGARD R, 595 (1972) 2.1-2.7.
- [4] F. Tejero Embuena, P. Doerffer, O. Szulc, Application of passive flow control device on helicopter rotor blades, Journal of the American Helicopter Society, (2015).

ACCEPTED MANUSCRIPT